Electric Field Effects on Relativistic Charged Particle Motion in Tokamaks

H.P.Zehrfeld, G.Fußmann,
and B.J.Green+)

IPP III/49 June 1979

MAX-PLANCK-INSTITUT FÜR PLASMAPHYSIK

8046 GARCHING BEI MÜNCHEN

MAX-PLANCK-INSTITUT FÜR PLASMAPHYSIK

GARCHING BEI MÜNCHEN

Electric Field Effects on Relativistic Charged Particle Motion in Tokamaks

H.P.Zehrfeld, G.Fußmann,
and B.J.Green+)

IPP III/49 June 1979

+) At present: JET Joint Undertaking
Culham Laboratory
Abingdon, Oxon., OX14 3EA
United Kingdom

Die nachstehende Arbeit wurde im Rahmen des Vertrages zwischen dem Max-Planck-Institut für Plasmaphysik und der Europäischen Atomgemeinschaft über die Zusammenarbeit auf dem Gebiete der Plasmaphysik durchgeführt.

IPP III/49

H.P. Zehrfeld
G. Fußmann
B.J. Green+)

Electric Field Effects on Relativistic Charged Particle Motion in Tokamaks

June 1979 (in English)

Abstract

We consider relativistic guiding center motion of charged particles (charge e, rest mass m_o) in magnetic fields consistent with toroidal tokamak equilibrium. The particle acceleration due to the toroidal electric field essential to tokamak operation, is taken into account. For the case of weak acceleration ($eU/m_oc^2 \ll 1$, where U is the loop voltage), the poloidal locus of charged particle motion is found to be an envelope of closed drift orbits at constant kinetic energy and is characterized by the existence of an appropriate adiabatic invariant. This allows, in the absence of collisions, a complete description of the motion and confinement of runaway electrons in tokamaks. For peaked current distributions and sufficiently high energies drift separatrices exist. They are calculated and their relevance to charged particle confinement and injection is considered.

+) At present JET Joint Undertaking,
Abingdon, Oxon., OX143EA,
England

1. Introduction

The study of relativistic runaway electrons has become the object of increasing interest. Such studies gain their particular importance from the fact that because of their quasi-collisionless motion runaway electrons may be experimentally used as test particles for the investigation of the confining magnetic field. In order to take advantage of this fact a theoretical analysis of collisionless runaway motion is an indispensible prerequisite.

The analysis is considerably simplified by a knowledge of the constants of motion. Charged particle motion in the axisymmetric magnetic field of an ideal tokamak is characterized by the constancy of the toroidal canonical momentum. Since through first order in gyroradius this extends to the toroidal canonical momentum of the guiding center /1/, guiding center motion in tokamak magnetic fields can be considered in terms of this constant and of the constants of motion E (energy) and μ (magnetic moment). Most calculations of runaway orbits in tokamaks are based on this approach (/2/, /3/ and references therein). For example, runaway orbits, with particle energy as a parameter, passing through a fixed point at the outside of the torus, have been calculated in /4/. From the experimental point of view the following more extended problem is of basic interest: what is the orbit of a runaway electron which is produced on a given magnetic surface after it has performed a very large number of toroidal revolutions (typically 10^6) and - by acceleration of the toroidal electric field essential to tokamak operation - has obtained an energy of the order of several MeV? This is the main problem treated in this paper. Our treatment takes account of the fact that runaway electrons increase their kinetic energy due to the accelerating force of the toroidal electric field. The presence of a toroidal electric field, of course, changes the situation with respect to the constants of motion. We consider time-independent electromagnetic fields, so that the magnetic moment μ and the total particle energy remain constant, but the corresponding Lagrangian now becomes a function of the toroidal angular coordinate so that the toroidal canonical angular momentum is no longer conserved. However, taking into account the smallness of eU/m_oc^2, which is the ratio of the particle one-turn energy gain to particle rest energy, the acceleration process is accompanied by only a quasistatic increase of the particle kinetic energy and the poloidal locus of charged particle motion is found to be an envelope of closed drift orbits at constant kinetic energy. The corresponding adiabatic invariant is derived in this paper.

Another important question is concerned with the change of runaway orbits due to a variation of plasma parameters such as profiles and absolute values of current and pressure. For example, in connection with the internal disruptions a sawtooth modulation in the hard X-ray intensity, produced by runaway electron bombardement of the limiter, has been observed in the Pulsator tokamak /5/. Here the question arises as to whether the observed modulations can be explained by the change of the runaway electron orbits due to a flattening of the current and pressure profiles. In order to treat this problem we consider magnetic fields consistent with toroidal tokamak equilibrium in terms of current and pressure distributions.

For nonflat current distributions and sufficiently high particle energies the occurrence of drift separatrices is observed. Their topology suggests charged particle injection into drift trajectories for the purpose of heating. Their geometry is calculated and the relevance to the problem of charged particle injection and of slowing-down is considered.

2. Basic Equations

We consider relativistic charged particle motion in terms of guiding center theory. The particle equation of motion averaged over the rapid revolution of a particle in its Larmor orbit gives the following equation for the time evolution of the guiding center position /7,8/

$$\frac{d\mathbf{x}}{dt} = \mathbf{v}_{\parallel} + \frac{1}{eB^2}\mathbf{B}\times\left\{\frac{m_0\gamma v_{\parallel}^2}{B^2}\mathbf{B}\cdot\nabla\mathbf{B} + \frac{m_0\gamma v_{\perp}^2}{2B}\nabla B - e\mathbf{E}\right\} \quad (1)$$

m_o and e are the particle rest mass and charge, respectively.

$$\mathbf{v}_{\parallel} = v_{\parallel}\frac{\mathbf{B}}{B}, \qquad \gamma \equiv \left(1-\frac{v^2}{c^2}\right)^{-1/2}, \text{ where } v^2 = v_{\parallel}^2 + v_{\perp}^2 \quad (2)$$

c is the speed of light, $\underline{E}$ is the electric and $\underline{B}$ the magnetic field.

We assume a time-independent electromagnetic field. In this case the electric field $\underline{E}$ has a potential Φ. The particle velocity components $v_{\parallel}$ and $v_{\perp}$ in equation (1) are related to the adiabatic invariant μ and the total particle energy E, which are constants of the motion, by

$$\mu = \frac{m_0\gamma^2 v_{\perp}^2}{2B}, \qquad E = m_0(\gamma-1)c^2 + e\Phi \quad (3)^{+)}$$

Taking into account that μ and E are constants of motion equation (1) can be re-written as

$$\frac{d\mathbf{x}}{dt} = \frac{1}{B}v_{\parallel}\left\{\left(1-\frac{m_0\gamma v_{\parallel}}{eB^3}\mathbf{B}\cdot\mathrm{rot}\,\mathbf{B}\right)\mathbf{B} + \frac{m_0}{e}\mathrm{rot}\left(\frac{\gamma v_{\parallel}}{B}\mathbf{B}\right)\right\} \quad (4)$$

where

$$v_{\parallel} = -\left\{1-\frac{1}{\gamma^2}\left(1+\frac{B}{B_0}(\gamma_0^2-1)\sin^2\alpha\right)\right\}^{1/2} c \quad (5)$$

$$\sin^2\alpha = \frac{2\mu B_0}{m_0c^2(\gamma_0^2-1)} \quad (6)$$

+) There are, with respect to the adiabatic expansion parameter m_o/e, some first order corrections of the magnetic moment. These, however, do not affect the validity of (1) expressed in terms of the constants of motion to this order, but concern the assignment of a particular value to μ for a particle whose initial position and velocity are given (see /1/).

$$\gamma = \gamma(E, \Phi(\mathbf{x})) = 1 + \frac{E - e\Phi(\mathbf{x})}{m_o c^2} \tag{7}$$

α is the angle+) between particle and magnetic field direction at some initial point $\underline{x}_o$, where B and γ have the values B_o and γ_o, respectively. The negative sign for $v_\parallel$ in (5) corresponds to the choice $\alpha \geqslant \pi/2$.

In what follows we consider the relativistic guiding center motion in an axisymmetric electromagnetic field appropriate to the ideal tokamak. This means that we include:

(A) magnetic fields consistent with toroidal tokamak equilibrium in terms of current and pressure distributions

(B) the toroidal electric field essential to tokamak operation.

Relativistic effects enter the guiding center motion according to (4) through (5)-(7). (A) means that the magnetic field and the current density are given by

$$\mathbf{B} = \nabla\xi \times \nabla G + \Lambda(G)\nabla\xi \tag{8}$$

$$\mu_o \mathbf{j} = \mathrm{rot}\,\mathbf{B} = \Lambda'(G)\nabla G \times \nabla\xi + R^2 \mathrm{div}\left(\frac{\nabla G}{R^2}\right)\nabla\xi \tag{9}$$

where G is the poloidal flux function determined by equilibrium in terms of current distribution $\Lambda(G)$ and pressure distribution p(G):

$$R^2 \mathrm{div}\frac{\nabla G}{R^2} + \Lambda\Lambda'(G) + 4\pi^2\mu_o R^2 p'(G) = 0 \tag{10}$$

A prime (') denotes the derivative of a function with respect to the given argument. ξ is the angle about the axis of symmetry divided by 2π, R is the distance from this axis. According to (B) we have the electric potential

$$\Phi(\mathbf{x}) = U\xi(\mathbf{x}) \tag{11}$$

where U is the loop voltage.

This last relation together with the equations (7-9) for the magnetic field give for the guiding center motion

$$\frac{d\mathbf{x}}{dt} = \frac{1}{B}v_\parallel\left\{\nabla\xi \times \left(\chi\nabla G - \frac{m_o}{e}\nabla\left(\frac{\gamma v_\parallel \Lambda}{B}\right)\right)\right\} + \frac{U}{4\pi^2 R^2 B^2}\nabla G + v\frac{V_\parallel}{B}\nabla\xi \tag{12}$$

+) For the interpretation of this angle the same qualifications have to be made as with respect to the magnetic moment.

where

$$\chi = 1 - \frac{m_o \gamma v_{\parallel}}{e B^3} \mathbf{B} \cdot \mathrm{rot}\, \mathbf{B} \tag{13}$$

$$\nu = \chi \Lambda + \frac{m_o}{e} \nabla G \cdot \nabla \left(\frac{\gamma v_{\parallel}}{B} \right) - \frac{m_o \gamma v_{\parallel}}{e B} \left(\Lambda \Lambda' + 4\pi^2 \mu_o R^2 p' \right) \tag{14}$$

$$\gamma = \gamma_o - \frac{e\mathcal{U}}{m_o c^2} \xi \,, \qquad \gamma_o = 1 + \frac{E}{m_o c^2} \tag{15}$$

and $v_{\parallel}$ is to be replaced according to (5).

3. Characteristic Features of the Motion

As all equilibrium scalars are independent of ξ , this angle variable is an "ignorable" co-ordinate in the sense that it enters each component of (12) only through γ according to equation (15). Therefore, if we use the time derivative of (15), equation (12) can be transformed into a purely poloidal problem and an equation describing the time evolution of γ :

$$\frac{d\mathbf{x}}{d\gamma} = - \frac{4\pi^2 R^2}{\nu} \frac{m_o c^2}{e\mathcal{U}} \nabla \xi \times \left\{ \chi \nabla G - \frac{m_o}{e} \nabla \left(\frac{\gamma v_{\parallel} \Lambda}{B} \right) \right\} - \frac{1}{\nu} \frac{m_o c^2}{e B v_{\parallel}} \nabla G \tag{16}$$

$$\frac{d\gamma}{dt} = - \frac{e\mathcal{U}}{m_o c^2} \frac{\nu v_{\parallel}}{4\pi^2 R^2 B} \equiv Q(\mathbf{x}, \gamma) \tag{17}$$

If $\underline{x} = \underline{c}(\underline{x}_o, \gamma)$ is a solution curve of (16) with $\underline{x}_o = \underline{c}(\underline{x}_o, \gamma_o)$, then solutions of the full problem lie on the rotation surface of $\underline{c}$, where $\gamma = \gamma(t)$ is implicitly determined by

$$t = t_o + \int_{\gamma_o}^{\gamma} \frac{d\gamma'}{Q(\mathbf{c}(\mathbf{x}_o, \gamma'), \gamma')} \tag{18}$$

and ξ is given by (15).

As a matter of fact, taking into account the smallness of $eU/m_o c^2$, which is the ratio of the particle one-turn energy gain to particle rest energy, relation (15) shows that $\gamma(t)$ is a slowly varying function of time in comparison with $\xi(t)$. Therefore we

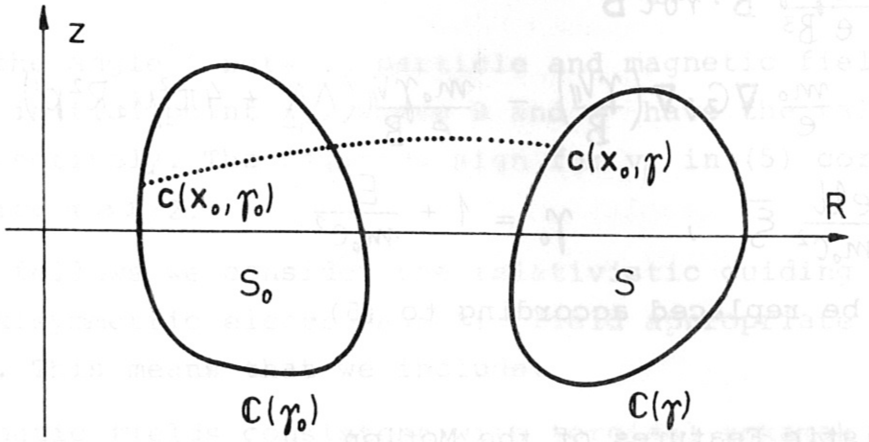

Fig. 1 Material lines for different values of γ together with a guiding center trajectory (dotted).

will retain the time parameter t, and consider $\gamma(t)$ as a weak function of time. Thus, instead of (16), we consider the poloidal problem

$$\frac{d\mathbf{x}}{dt} = \frac{1}{B} V_{\parallel} \nabla\xi \times \left\{ \chi \nabla G - \frac{m_0}{e} \nabla\left(\frac{\gamma V_{\parallel} \Lambda}{B}\right) \right\} + \frac{\mathcal{U}}{4\pi^2 R^2 B^2} \nabla G \equiv V(x,t) \quad (19)$$

Solutions of this equation obviously represent the trace of guiding center motion in a poloidal plane.

Let us, for some initial time $t=t_o$ with $\gamma_o = \gamma(t_o)$, consider a drift particle ensemble on an arbitrary closed poloidal curve $\mathbb{C}(\gamma_o)$. The poloidal trace of each drifting particle initially lying on $\mathbb{C}(\gamma_o)$ with increasing $\gamma = \gamma(t)$ moves along one of the above-mentioned solution curves $\underline{x} = \underline{c}(\underline{x}_o, \gamma(t))$, and the poloidal loci of the positions of all such particles for a given value of γ constitute a closed poloidal curve $\mathbb{C}(\gamma)$ (see Fig.1). In hydrodynamics such curves which are carried by the poloidal flow $\underline{V}(\underline{x},t)$ are called material lines /9/. The rate of change of the area S enclosed by such a material line by purely kinematic considerations is given by

$$\frac{1}{2\pi} \frac{dS}{dt} = \oint_{C(\gamma)} R(\nabla\xi \times V(x,t)) \cdot dx \quad (20)$$

Now any poloidal axisymmetric velocity field $\underline{V}(\underline{x},t)$ can be represented as

$$\mathbf{V} = W\,\nabla\xi \times \nabla G^* \tag{21}$$

where W and G are two scalar functions determined by the flow field $\underline{V}(\underline{x},t)$. The introduction of the representation (21) into (20) gives

$$\frac{dS}{dt} = -\frac{1}{2\pi}\oint_{C(\gamma)} \frac{W}{R}\,\nabla G^* \cdot d\mathbf{x} \tag{22}$$

If G^* is single-valued and the function W turns out to be of the form $W = C.R$, where C is a constant, then the considered flow is area preserving in the sense that the area enclosed by poloidal contours carried by the flow is constant. The tokamak equilibria we wish to consider satisfy the above conditions for the functions W and G^* , so that relativistic guiding center flow is characterized by that property.

In the case of weak electric fields ($eU/m_oc^2 \ll 1$) we get from this property, besides the constants of motion E and μ, a third geometrical one as follows:

In concepts of motion of a continuous medium any particular poloidal guiding center trajectory $\underline{x} = \underline{c}(\underline{x}_o,\gamma)$, by the definition of stream lines, can be interpreted as the envelope of the one-parameter family of stream lines through the points constituting this trajectory. The parameter is γ and the stream line corresponding to a particular value of γ consists of the points $\underline{x}'$ satisfying the equation $G^*(\underline{x}',\gamma) = G^*(\underline{c}(\underline{x}_o,\gamma),\gamma)$. We especially refer to situations with closed stream lines. Due to the smallness of the parameter eU/m_oc^2 each member of such a family of closed stream lines, for times involving a sufficiently small variation of γ , is an almost perfect representative of the guiding center trajectory itself and for this reason also of a material line. Therefore the real guiding center motion becomes the envelope of such closed level surfaces of the function G^*, whose cross-sectional area is constant, i.e. this cross-sectional area becomes a constant of motion in the sense of an adiabatic invariant. By methods of classical mechanics (e.g. /10/) the latter can be shown by performing a corresponding time average of dS/dt using $W = C.R$ for the motion (21). As the derivation is standard we omit an explicit proof, but in the appendix give an example, where the exact motion is known and the character of the adiabatic approximation can be very clearly seen.

4. Curvature, Plasma and Electric Field Effects on Particle Drifts

A treatment of the full problem would consist (a) in the consideration of a particular plasma equilibrium with prescribed pressure and current distributions and (b), on the basis of the resulting equilibrium magnetic field, in a solution of the equations (12) to (15), whose free parameters are the loop voltage U, the total particle energy E and the initial pitch angle α.

In order to simplify the equilibrium part of the problem we make use of the customary approach to tokamak equilibrium and consider equation (10), the equation for the poloidal magnetic flux, in a large aspect-ratio approximation which gives results correct to first order in inverse aspect-ratio /11/. The magnetic surfaces are represented by non-concentric tori of circular cross-section. These, and the co-ordinates naturally associated with them, are illustrated in fig. 2.

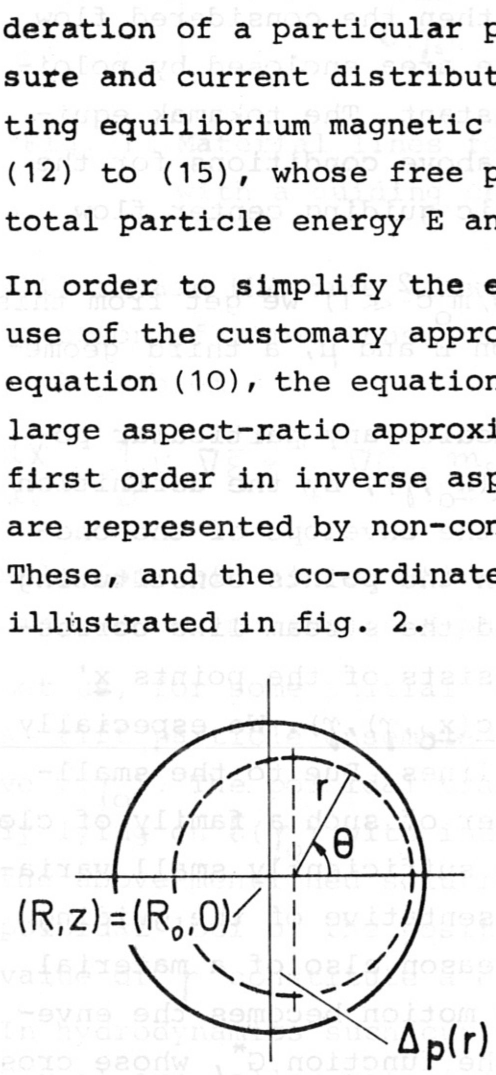

Fig. 2 Illustration of the relation between R-z and r-θ co-ordinates determined by the displacement function Δ_p.

For pressure and toroidal current we assume the following class of distributions

$$p = p_0 (1-\rho^2)^n \qquad (23)$$

$$I = I_T \left\{ 1 - (1-\rho^2)^{m+1} \right\} \qquad (24)$$

where $\rho = r/a$, a the small plasma radius, p_o the plasma pressure on the magnetic axis+) and I_T the total toroidal plasma current. n and m are arbitrary positive integer exponents++) describing the peakedness of the distributions.

Poloidal flux G and plasma displacement Δ_p are then given by

$$G = \frac{1}{2}\mu_o R_o I_T \cdot F_{m+1}(x) \tag{25}$$

$$\frac{\Delta_p}{a} = \frac{a}{2R_o}\int_0^{1-\rho^2} F(x')\,dx' \equiv \Delta(\rho) \tag{26}$$

where

$$x = 1-\rho^2 \tag{27}$$

$$F_{m+1}(x) = \sum_{k=1}^{m+1} \frac{1}{k}(1-x^k) \tag{28}$$

$$F(x) = \beta_p \cdot \frac{1+nx^{n+1}-(n+1)x^n}{(1-x^{m+1})^2} + \frac{F_{m+1}(x)-\frac{1}{2}F_{2(m+1)}(x)}{(1-x^{m+1})^2} \tag{29}$$

$$\beta_p = \frac{8\pi^2 a^2 p_o}{(n+1)\mu_o I_T^2} \tag{30}$$

is the poloidal beta at the boundary of the plasma.

The toroidal current density corresponding to the distributions (23) and (24) is

$$j_T = \frac{I_T}{\pi a^2}\left\{\frac{1}{2}\beta_p n\cdot(n+1)\frac{(1-x)x^{n-1}}{1-x^{m+1}}\frac{R^2-R_o^2}{RR_o} + (m+1)x^m\frac{R_o}{R}\right\} \tag{31}$$

According to our considerations in the preceding section the poloidal trace of a guiding center orbit is given by a solution of the equations (19) and (17) which we re-write as follows:

$$\frac{d\mathbf{x}}{dt} = \frac{1}{B}v_\parallel \nabla\xi \times \nabla G^* + \frac{(\gamma-1)v_\parallel}{B}\nabla\xi\times\nabla G + \frac{\mathcal{U}}{(2\pi RB)^2}\nabla G \tag{32}$$

$$\frac{d\gamma}{dt} = -\frac{e\mathcal{U}}{m_o c^2}\cdot\frac{v v_\parallel}{4\pi^2 R^2 B} \tag{33}$$

+) Note that the same subscript 'o' has different meanings depending on the quantity to which it is attached.

++) The restriction to integer values is not essential.

where
$$G^* = G^*(\mathbf{x},\gamma) = G - \frac{m_o \gamma v_\parallel}{eB} \Lambda(G) \tag{34}$$

For a determination of the functions χ, ν and $v_\parallel$ entering these equations we have to consider the relations (13), (14) and (5). In the large aspect-ratio approximation, using (9) in (13), we obtain for

$$\chi = 1 - \frac{1}{A^2}\frac{v_\parallel}{c} \cdot \frac{\gamma I_A}{q^2 I_T}(m+1)x^m + O\left(\frac{1}{A^3}\right) \tag{35}$$

$$A = \frac{R_o}{a}, \qquad q = \frac{2\pi a^2 B_{TO}}{\mu_o I_T R_o}, \qquad I_A = \frac{4\pi m_o c}{\mu_o e} \tag{36}$$

with aspect-ratio A, B_{TO} toroidal magnetic field on axis, safety factor q and Alfven current I_A. Thus the second term in (32) is of second order in inverse aspect-ratio and therefore removed from the present consideration.

The last term in (32) is in magnitude $U/\mu_o I_T A^2 q v_\parallel$ times smaller than the first one. As we consider only unidirectional motion of guiding centers with particle energies $E > kT/m_o$, this term, which is the ExB-term, is negligibly small for typical tokamak parameters.

Thus, instead of (32), we consider

$$\frac{d\mathbf{x}}{dt} = \frac{e\Delta^*}{m_o \gamma q A} R\, \nabla\xi \times \nabla G^* \tag{38}$$

where
$$G^* = G - \mu_o I_T A \Delta^* R \tag{39}$$

$$\Delta^* = \frac{\gamma}{2A}\frac{I_A}{I_T}\frac{v_\parallel}{c} \tag{40}$$

$$R = R_o\left(1 + \frac{1}{A}(\rho\cos\theta + \Delta(\rho))\right) \tag{41}$$

and G and $v_\parallel$ are given by (25) and (5), respectively. In order to exclude terms of second order in inverse aspect-ratio from consideration we must limit the initial pitch angle such that $A.\sin^2\alpha < 1$. From (5) and (40) we obtain then that the coefficient of the vector product in (38) is proportional to R.

Therefore the function W, introduced for the representation (21) of the poloidal guiding center flow field, is indeed of the form required for an area-preserving material motion. As we have shown in the last section this means that particles lying at some moment of time on a closed toroidal surface (e.g. a magnetic surface) move in such a manner that the cross-sectional area of the corresponding material surface remains constant.

Before making use of this property we go into a closer consideration of the level surfaces of the function G^*, which in fact are drift surfaces at constant kinetic energy. They can be easily illustrated by adding to the (R,z)-co-ordinates of a poloidal plane a third, auxiliary one labelling a stack of parallel (R,z)-planes in upward direction. As such a co-ordinate we take the value G of the poloidal magnetic flux and consider (39) in the resulting (R,z,G)-space. In this space the poloidal flux function (25) is represented by a bell-shaped surface and, for particular values of G^* and γ, relation (39) can be interpreted as an equation for the intersection of this bell-shaped surface with the plane $G = G^* + \mu_o I_T A \Delta^* R$. The projection of this intersection onto the the actual poloidal plane characterizes then a level surface of G^*. The direction of the intersecting planes, for given plasma parameters, is determined by the value of Δ^*, i.e. by γ and α; for $\gamma = 1$, that is the case of horizontal planes, magnetic and drift surfaces coincide.

With increasing γ magnetic and drift surfaces through a given point in the actual (R,z)-plane differ from each other more and more and we expect conditions for the closure of the latter.

Analytically, level surfaces of (39) through the outermost point $(\rho,\Theta) = (\lambda,0)$ of the magnetic surface with the (normalized) radius λ (fig. 3) must satisfy the equation

$$\Delta^*(\rho\cos\theta - \lambda + \Delta(\rho) - \Delta(\lambda)) = \frac{1}{2}\left\{F_{m+1}(x(\rho)) - F_{m+1}(x(\lambda))\right\} \tag{42}$$

They are closed in the circular region $0 \leq \rho \leq 1$ if the function Δ^* is such that

$$\Delta^*(\gamma,\alpha) < \Delta^*_s(\lambda) \equiv \frac{1-(1-\lambda^2)^{m+1}}{\lambda(1+\Delta'(\lambda))} \tag{43}$$

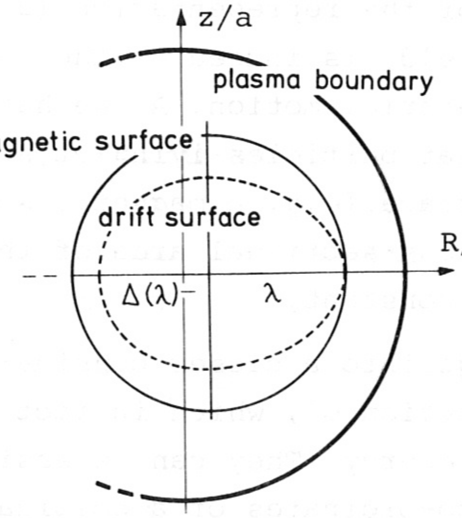

Fig. 3 The geometry of magnetic and relativistic particle drift surfaces through a given point $(R,z) = (R_o+a(\lambda+\Delta(\lambda)),0)$ in a poloidal plane.

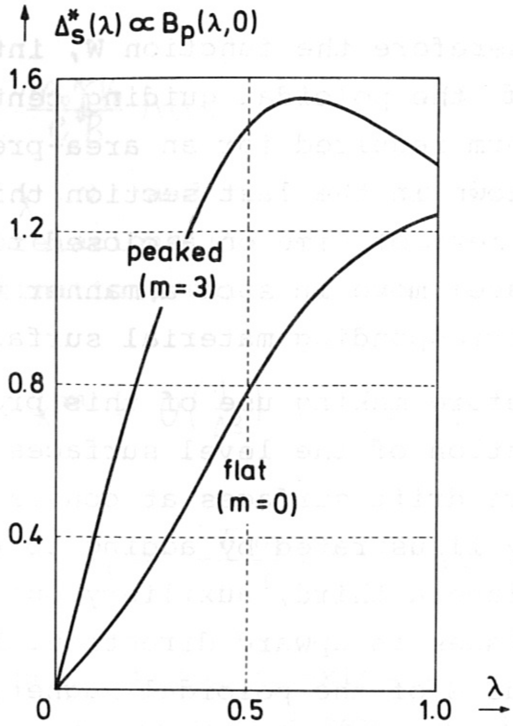

Fig. 4 The dependence of Δ_s^* on the radial parameter λ .

$\Delta'(\lambda)$ is the derivative of Δ at $\rho=\lambda$ and according to (26) given by

$$\Delta'(\lambda) = -\frac{\lambda}{A} F(x(\lambda)) \tag{45}$$

The right-hand side of (43), which is proportional to the poloidal magnetic field as a function of the radial parameter λ,

$$\Delta_s^*(\lambda) = \frac{B_p(\lambda,0)}{(1+\Delta'(1))\, B_p(1,0)} \tag{46}$$

is plotted in fig. 4 for a flat and for a peaked current distribution. Fig. 4 illustrates the fact that for nonflat current distributions there is a finite region inside of the outermost magnetic surface with radially decreasing poloidal magnetic field. Closer investigation of the contour equation (42) reveals that, for kinetic energies $E_k = m_o(\gamma-1)c^2$ such that

$$\Delta^*(\gamma,\alpha) = \Delta_s^*(\lambda) \tag{47}$$

applies, which, in detail, means

$$\frac{(\gamma^2-1)^{1/2}}{2A}\,\frac{I_A}{I_T}\left\{1-\frac{\gamma_o^2-1}{\gamma^2-1}\sin^2\alpha\right\}^{1/2} + \frac{1-(1-\lambda^2)^{m+1}}{\lambda(1+\Delta'(\lambda))} = 0 \;, \tag{47'}$$

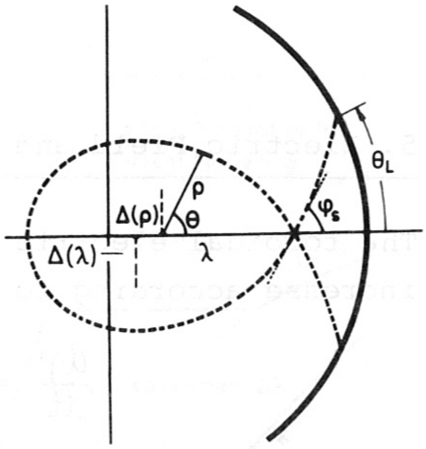

Fig. 5 The geometrical parameters of stagnation point and drift separatrix.

a stagnation point appears at $(R,z) = (R_o+a(\lambda+\Delta(\lambda)),0)$. Fig. 5 shows the geometry of the corresponding drift separatrix. The angle between the plane z=0 and the plane tangent to the drift surface through the stagnation point can be calculated from

$$(1+\Delta'(\lambda)) \cdot tg^2\varphi_S = 1 - \frac{2(m+1)\lambda^2(1-\lambda^2)^m}{1-(1-\lambda^2)^{m+1}} \tag{48}$$

The angle Θ_L for which particles leave or enter the plasma at the boundary can be calculated using formula (42):

$$\cos\Theta_L = \lambda + \Delta(\lambda) + \frac{1}{2\Delta_S^*}\left\{F_{m+1}(0) - F_{m+1}(x(\lambda))\right\} \tag{49}$$

$|\Theta_L|$ has its maximum for maximum Δ_S^*, i.e. for maximum poloidal magnetic field in the plane z=0.

Associated with this angle are two others describing the geometry of the separatrix at the plasma boundary: The angle φ_p between the inward normal to the plasma boundary and the poloidal velocity field direction there, and the angular deflection φ_T of the particle trajectory direction from the toroidal direction in $(\rho,\Theta) = (1,\Theta_L)$. For these two angles it is found:

$$\cos\varphi_p = \frac{\Delta_S^* D_L \sin\theta_L}{(1-2\Delta_S^* D_L\cos\theta_L + (\Delta_S^* D_L)^2)^{1/2}} \tag{50}$$

$$tg\,\varphi_T = \frac{(1-2\Delta_S^* D_L\cos\Theta_L + \Delta_S^{*2} D_L^2)^{1/2}}{qA\,D_L} \tag{51}$$

where $$D_L \equiv 1 + \Delta'(1)\cdot\cos\theta_L \tag{52}$$

5. Electric Field and Current-Flattening Effects on Runaway Motion

The toroidal electric field typical for a tokamak causes γ to increase according to

$$\frac{d\gamma}{dt} = - \frac{eU}{m_o c^2} \frac{I_T}{I_A} \frac{A\Delta^*}{\pi\gamma} \frac{c}{R} \tag{53}$$

This expression is obtained employing in the considered approximation the equations (33), (14), (37) and (40). For electrons, due to the smallness of $eU/m_o c^2$, this acceleration process is accompanied by only a quasistatic increase of the particle kinetic energy. Therefore, together with the stated area-preserving property of material motion, charged particles on closed drift orbits move around members of that subset of level surfaces of G^*,

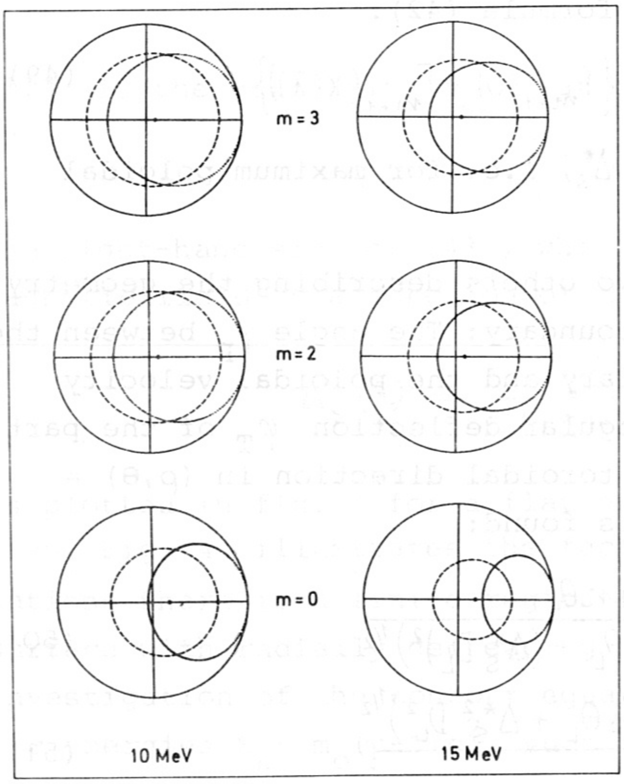

Fig. 6 Runaway electrons of 10 MeV and 15 MeV, respectively, on drift surfaces touching the limiter. These electrons originate on magnetic surfaces (indicated by dashed lines).

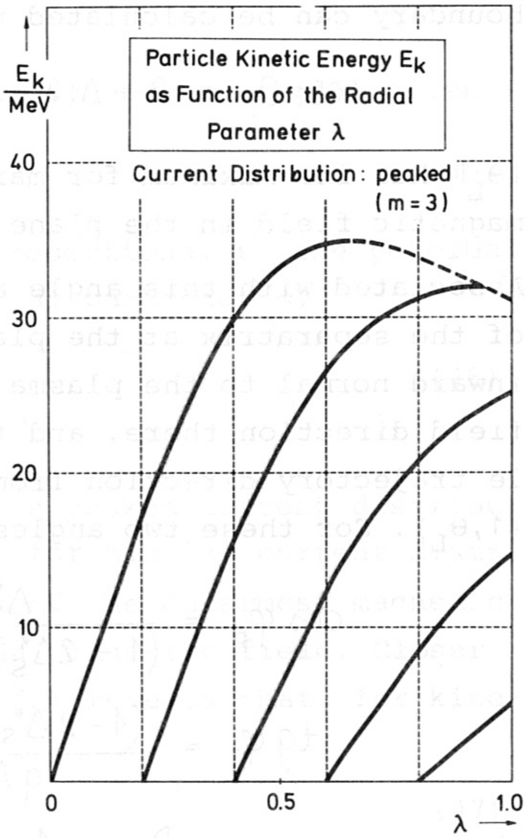

Fig. 7 The λ-values for E_k=0 are equal to the normalized radii of the magnetic surfaces on which runaway electrons of given energy originate.

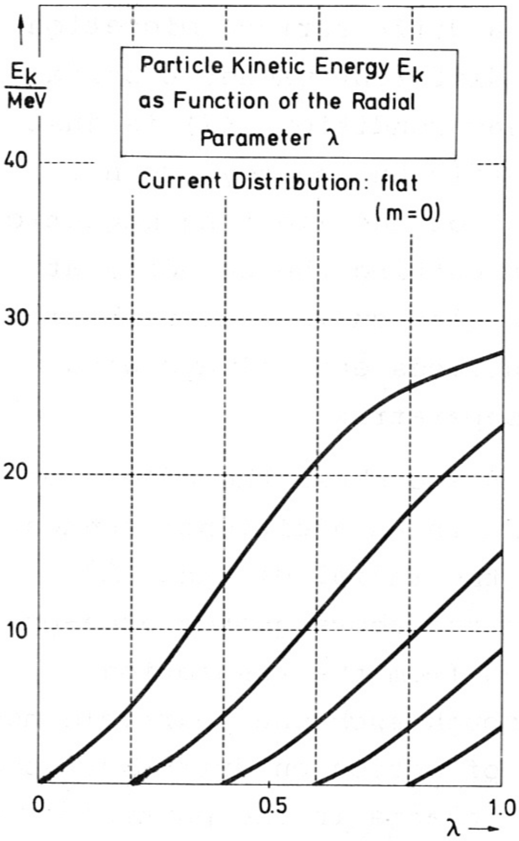

Fig. 8 As fig. 7, but for a flat current distribution.

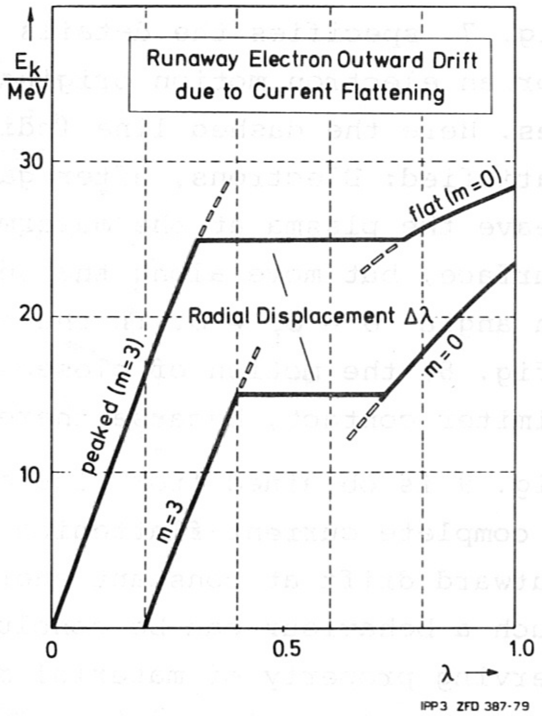

Fig. 9 Radial displacement of electrons at a given energy (15 MeV and 25 MeV, respectively) due to current-flattening.

whose cross-sectional area is constant. Thus charged particle motion in a weak toroidal electric field establishes an equivalence relation between usual drift surfaces of different energy and position which can be interpreted as a drift surface motion. Figures 6-9 illustrate this characteristic feature of weakly accelerated charged particle motion for a particular case+). In fig. 6 runaway electrons of given energy are observed in their motion on drift surfaces touching the limiter. Figures in different rows correspond to current distributions of different peakedness (m = 0, 2 and 3). Together with these drift surfaces the magnetic surfaces of equal cross-sectional area are given (dashed lines), i.e. the locus on which runaway electrons originate at the beginning of the acceleration process.

+) We refer to some calculations for the tokamak PULSATOR, for which we have taken the following data: $R_O = 0.70$ m, $a = 0.11$ m $I_T = 60$ kA, $B_{TO} = 3$ T, $n = 3$, $\beta_p = 1.01$.

Fig. 7 specifies the details of such a drift surface migration for an electron motion originating on different magnetic surfaces. Here the dashed line indicates that condition (47) is just satisfied: Electrons, after gaining sufficient energy, do not leave the plasma at the outermost point of the limiting magnetic surface, but move along the separatrix cutting the boundary at an angle $\theta = \theta_L \neq 0$. In the case of a flat current distribution (fig. 8) the motion of closed drift surfaces ends always with limiter contact, because there is no separatrix.

Fig. 9 is obtained from figures 7 and 8 and shows the effect of a complete current-flattening resulting in an additional runaway outward drift at constant energy over the radial distance $\Delta\lambda$. Such a behaviour can be concluded from the above-quoted area-preserving property of material motion and from the assumption that the flattening process is slow enough such that particle motion can still be considered in terms of motion on drift surfaces, but fast enough to have no significant change in the particle kinetic energy.

6. The Problem of Charged Particle Injection and of Slowing-Down

In the absence of a toroidal electric field and for constant particle energy the equations (1) represent the usually considered drift equations. For the large aspect-ratio approximation of the equilibrium magnetic field treated above their solutions are the object of our investigations for the case U=0. As we have seen, for sufficiently high particle energies, in regions with radially decreasing poloidal magnetic field, a stagnation point and a drift separatrix appear. Depending on the stagnation point position λ the corresponding particle energies can be obtained from condition (47). Putting $\gamma_0 = \gamma$, equation (47) gives for the energy $E_k = m_o(\gamma-1)c^2$

$$E_k = \left\{\left[1 + \left(\frac{2A\,\Delta_s^*(\lambda)}{\cos\alpha}\,\frac{I_T}{I_A}\right)^2\right]^{1/2} - 1\right\} m_o c^2 \tag{54}$$

Neglecting plasma displacement and pitch angle effects this sim-

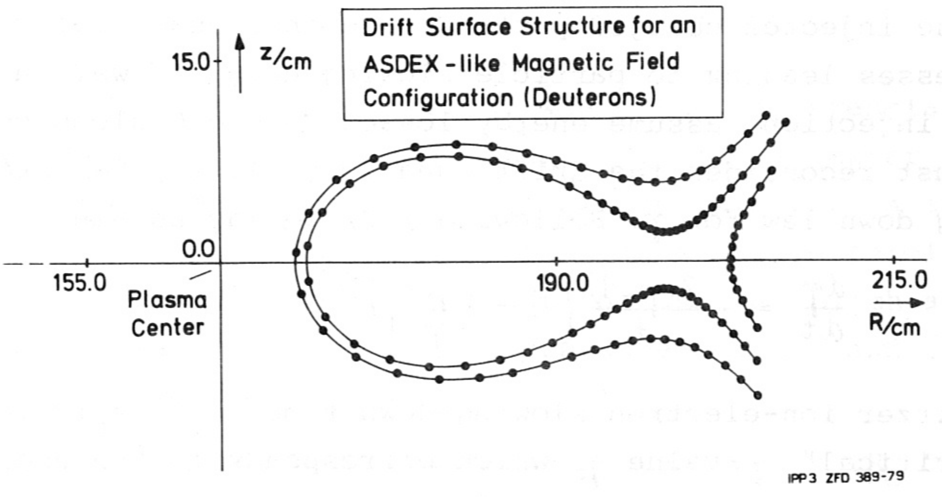

Fig. 10

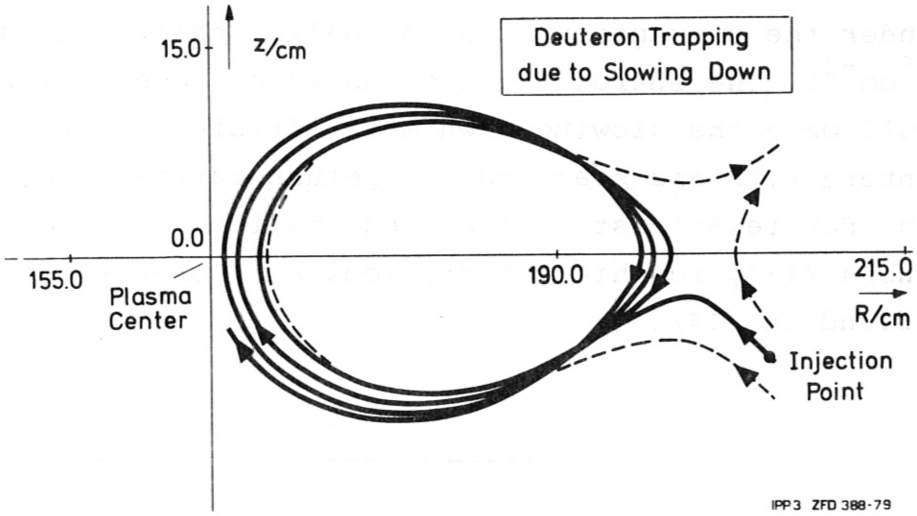

Fig. 11

plifies to $E_k/\text{MeV} = \Delta_s^*.A.I_T/16.7$ for relativistic electrons and to $E_k/\text{eV} = 1.93.(A.\Delta_s^*.I_T.Z)^2/M$ for nonrelativistic ions (Z is the ion charge and M the mass number, I_T in kA), where Δ_s^*, according to equation (46), is given by $\Delta_s^* = B_p(R_o+a.\lambda,0)/B_p(R_o+a,0)$. For an ASDEX-like magnetic field configuration, for example, we find for electrons 74-103 MeV, for deuterons 1.5-2.9 MeV (I_T = 300 kA). Fig. 10 shows the resulting drift surfaces for deuterons with an energy of 2 MeV ($\alpha = 0$, $\Delta_p = 0$, m=3; 12 orbital points correspond to one toroidal turn). Their geometry with trajectories leading from the boundary into the plasma suggests charged particle injection for the purpose of heating. The heating effectiveness of the injected charged particles depends essentially on the processes leading to particle slowing-down. If we, in the case of ion injection, assume energy losses due to Coulomb collisions, we must reconsider the drift equations (1) supplemented by a slowing down law for γ. Following /12/ we may assume

$$\frac{d\gamma}{dt} = -\frac{2(\gamma-1)}{t_s}\left\{1+\left(\frac{\gamma_c-1}{\gamma-1}\right)^{3/2}\right\} \tag{55}$$

with the Spitzer ion-electron slowing-down time $t_s = t_s(T_e, n_e)$ and some "critical" γ-value γ_c which corresponds to the energy, where the differential energy transfer to the ions equals that to the electrons. Solving the corresponding differential equations we can achieve deuteron trapping as illustrated in Fig. 11, however, only under the assumption of an unrealistically high density ($n_e = 10^{16}\,\mathrm{cm}^{-3}$). The introduction of anomalous energy loss processes would make the slowing-down more efficient. Here particle-wave interaction and beam-induced return currents come into question. For relativistic electrons the importance of these effects is known /13/, for high-energy ions a theoretical treatment can be found in /14/.

Appendix

We consider a particular case, where the differential equations (16) for the poloidal trace of guiding center trajectories allow an analytical solution which facilitates a quantitative investigation of the effect of a finite toroidal electric field on the motion. We put the initial pitch angle equal to zero, neglect plasma pressure effects and consider a flat current distribution (m = 0).

Written in polar co-ordinates about the origin $(R_o, 0)$ in a poloidal plane the equations (16) read

$$\frac{d\rho}{d\gamma} = \omega\,\Delta^*(\gamma)\cdot \sin\theta \tag{A1}$$

$$\frac{d\theta}{d\gamma} = \frac{\omega}{\rho}\left(\Delta^*(\gamma)\cdot\cos\theta - \rho\right) \tag{A2}$$

where ρ is normalized by $\rho = r/a$ and Δ^* and ω are given by

$$\Delta^*(\gamma) = -\frac{I_A}{2AI_T}\left(\gamma^2-1\right)^{1/2} \tag{A3}$$

$$\omega = \frac{2\pi m_o c^2}{e\mathcal{U}q} = \frac{\omega_P}{\Delta\omega_T} \tag{A4}$$

For orbits closed in the considered region, ω can be interpreted as the ratio of the frequency ω_p of poloidal revolution to the increase $\Delta\omega_T$ in the toroidal revolution frequency ω_T during one toroidal orbit due to acceleration.

If in the R-z plane we introduce other polar co-ordinates (ρ^*, θ^*) about the origin $(R,z) = (R_o + a.X(\gamma), a.Z(\gamma))$, which is shifted with respect to the original one by the γ-dependent distance $a.(X^2+Z^2)^{1/2}$, then the equations

$$\frac{d\rho^*}{d\gamma} = 0 \tag{A5}$$

$$\frac{d\theta^*}{d\gamma} = -\omega \tag{A6}$$

are equivalent to (A1,A2), if the new origin satisfies the equations

$$\frac{dX}{d\gamma} = \omega Z \tag{A7}$$

$$\frac{dZ}{d\gamma} = \omega(\Delta^* - X) \tag{A8}$$

Using at $\gamma = \gamma_0$ the initial conditions

$$X(\gamma_0) = \Delta^*(\gamma_0) \tag{A9}$$

$$Z(\gamma_0) = 0 \tag{A10}$$

the solution of the system (A7,A8) is given by

$$X(\gamma) = \Delta^*(\gamma_0) + \omega \cdot \int_{\gamma_0}^{\gamma} (\Delta^*(\gamma') - \Delta^*(\gamma_0)) \cdot \sin \omega(\gamma - \gamma')\, d\gamma' \tag{A11}$$

$$Z(\gamma) = \omega \cdot \int_{\gamma_0}^{\gamma} (\Delta^*(\gamma') - \Delta^*(\gamma_0)) \cdot \cos \omega(\gamma - \gamma')\, d\gamma' \tag{A12}$$

The flow associated with the kinematic equations (A1,A2) is nonstationary if $U \neq 0$. Its stream lines are given by the level surfaces of G^* according to equation (39). They turn out to be concentric circles about the center $(R,z) = (R_o + a.\Delta^*(\gamma), 0)$.

The equations (A5) and (A6) show that - regardless of the loop voltage-driven time-dependence of the accelerated co-ordinate system (ρ^*, θ^*) - any closed contour carried by the flow experiences a rigid rotation by the angle $-\omega(\gamma(t) - \gamma_0)$, so that the flow is area-preserving in the sense of our explanations in section 3.

To investigate the nonstationary character and the geometry of the flow we focus our attention on the dependence on the loop voltage, i.e. on ω.

For sufficiently high energies the integrals (A11,A12) are easy to evaluate. For $\gamma^2 \gg 1$ (A3) gives

$$\Delta^*(\gamma) = \varkappa \gamma \ , \quad \text{, where} \quad \varkappa = -\frac{I_A}{2 A I_T} \tag{A13}$$

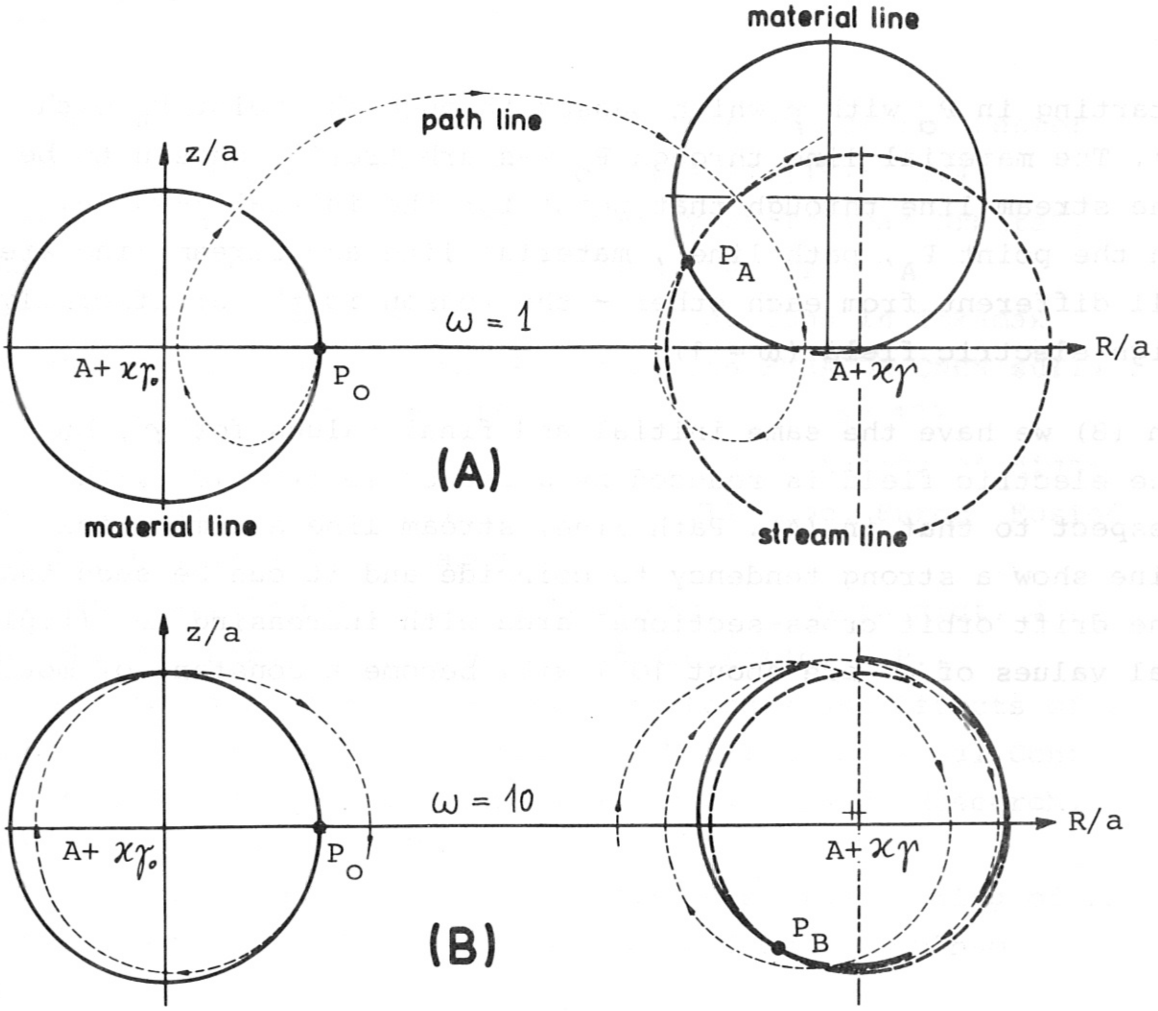

Fig. A1 Path lines, material lines and stream lines for an analytical solution of the relativistic drift equations. In (B) the electric field is reduced by a factor 10 with respect to that in (A).

and the integrations in (A11) and (A12) give for $X(\gamma)$ and $Z(\gamma)$

$$X(\gamma) = \varkappa\left(\gamma - \frac{1}{\omega}\sin\omega(\gamma-\gamma_0)\right) \tag{A14}$$

$$Z(\gamma) = \frac{\varkappa}{\omega}\left(1 - \cos\omega(\gamma-\gamma_0)\right) \tag{A15}$$

The figure illustrates the motion associated with (A14) and (A15). The first case (A) shows a path line (indicated by arrows) starting in P_o with γ_o which passes through the point P_A with γ. The material line through P_o was arbitrarily chosen to be the stream line through that point for the initial γ-value. In the point P_A, path line , material line and stream line are all different from each other - the reason is the artificially high electric field ($\omega = 1$).

In (B) we have the same initial and final values for γ , but the electric field is reduced by a factor 10 ($\omega = 10$) with respect to that in (A). Path line, stream line and material line show a strong tendency to coincide and it can be seen that the drift orbit cross-sectional area with increasing ω (typical values of ω are about 10^5) will become a constant of motion.

Literature

1. Northrop, T.G., Rome, J.A., "Extensions of Guiding Center Motion to Higher Order", Phys. Fluids 21 (1978) 384
2. Rome, J.A., Peng, Y.K., "The Topology of Tokamak Orbits", Oak Ridge National Laboratory, ORNL/TM-6352
3. Knöpfel, H., Spong, D.A., "Runaway Electrons in Tokamak Discharges", Report of the Associazione EURATOM-CNEN sulla Fusione, Centro di Frascati, 77.24/p, November 1977
4. Knöpfel, H., Spong, D.A., Zweben, S.J., "Dynamics of High-Energy Runaway Electrons in ORMAK", VII Proc. Europ. Fusion Conf., Lausanne 1975, paper 3
5. Fußmann, G., Engelhardt, W., Feneberg, W., Gernhardt, J., Glock, E., Karger, F., Sesnic, S., Zehrfeld, H.P., "Investigation of Modulated Runaway Losses and Effects of a Helical Dipole Field in Pulsator", VII International Conf. on Plasma Physics and Controlled Nuclear Fusion Research, Innsbruck 1978, IAEA-CN-37-T4
6. Hugill, J., Appendix A1 of "Neutral Injection Heating of Toroidal Reactors", CLM-R 112, a report from the Culham Study Group, 1971
7. Morozov, A.I.,Solov'ev, L.S., "Integrals of the Drift Equations", DAN 128, 3, 506 (1959).
8. Morozov, A.I., Solov'ev, L.S., "Reviews of Plasma Physics", Vol. 2, Cons. Bureau, New York, 1966, p. 227
9. Truesdell, C., Toupin, R., "The Classical Field Theories" in "Handbuch der Physik", Vol. III/1, p. 339, Springer Verlag, 1960
10. Landau, L.D., Lifschiz, E.M., in "Mechanik", Akademie-Verlag, Berlin, 1962, p. 180
11. Shafranov, V.D., "Reviews of Plasma Physics", Vol. 2, Cons. Bureau, New York, 1966, p. 102
12. Stix, T.H., Plasma Physics 14 (1971), 367
13. Benford, J. et al., Intern. Conf. on Plasma Physics and Contr. Thermon. Fusion, Berchtesgaden (1976), IAEA-CN-35/G2-3
14. Sudan, R.N., Phys. Rev. Lett. 37, 24 (1976), 1613